Raman spectroscopic study of the magnesium carbonate mineral– hydromagnesite $Mg_5[(CO_3)_4(OH)_2]\cdot 4H_2O$
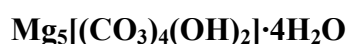
Ray L. Frost [•]

Chemistry Discipline, Faculty of Science and Technology, Queensland University of Technology, GPO Box 2434, Brisbane Queensland 4001, Australia.

Abstract

Magnesium minerals are important for the understanding of the concept of geosequestration. One method of studying the hydrated hydroxy magnesium carbonate minerals is through vibrational spectroscopy. A combination of Raman and infrared spectroscopy has been used to study the mineral hydromagnesite. An intense band is observed at 1121 cm^{-1} attributed CO_3^{2-} ν_1 symmetric stretching mode. A series of infrared bands at 1387, 1413, 1474 cm^{-1} are assigned to the CO_3^{2-} ν_3 antisymmetric stretching modes. The CO_3^{2-} ν_3 antisymmetric stretching vibrations are extremely weak in the Raman spectrum and are observed at 1404, 1451, 1490 and 1520 cm^{-1}. A series of Raman bands at 708, 716, 728, 758 cm^{-1} are assigned to the CO_3^{2-} ν_2 in-plane bending mode. The Raman spectrum in the OH stretching region is characterised by bands at 3416, 3516 and 3447 cm^{-1}. In the infrared spectrum a broad band is found at 2940 cm^{-1} assigned to water stretching vibrations. Infrared bands at 3430, 3446, 3511, 2648 and 3685 cm^{-1} are attributed to MgOH stretching modes.

KEYWORDS: Geosequestration of greenhouse gases; Magnesium Carbonate; $(CO_3)^{2-}$; hydromagnesite, Raman spectroscopy

---

[•] Author to whom correspondence should be addressed (r.frost@qut.edu.au)

INTRODUCTION

Hydromagnesite $Mg_5[(CO_3)_4(OH)_2]\cdot 4H_2O$ is a low temperature hydrothermally formed mineral [1-3]. Under natural conditions, hydromagnesite may form in evaporites depending on the availability of the Mg^{2+} ions in solution in relation to the availability of other cations such as Ca^{2+}. [1] The highly hydrated nature of the Mg^{2+} ion prevents the formation of anhydrous $MgCO_3$ phases [2]. Additionally hydromagnesite can form as efflorescences on existing carbonate rocks, man-made bricks and mortars, serpentinites, volcanic breccias and even meteorites [4-8]. The conditions of formation are claimed to be independent of the carbon dioxide partial pressure [1] but are probably pH dependent. The mineral is also formed in caves from water that has seeped through Mg-rich rocks [8]. It is sometimes called 'moon milk'.

The formation of carbonates such as hydromagnesite may be a key to the sequestration of carbon dioxide [9, 10] i.e. the removal of greenhouse gases from the atmosphere. The study of the carbonates of magnesium is of high importance in the development of technology for the removal of greenhouse gases. Magnesium minerals such as brucite, periclase and hydrotalcites have the potential for the sequestration of carbon dioxide. The formation and reaction pathways of hydroxy and hydrous carbonates of magnesium are essential for the understanding of this sequestration. The hydration-carbonation or hydration-and-carbonation reaction path in the MgO-CO_2-H_2O system at ambient temperature and atmospheric CO_2 is of essential significance from the standpoint of carbon balance and the removal of greenhouse gases from the atmosphere. A better understanding of the global masses of Mg and CO_2 and the thermal stability of the hydrated carbonates of magnesium will provide a practical understanding for carbon dioxide removal. From a practical point of view, the exact knowledge of the reaction path in MgO-CO_2-H_2O system is of great significance to the performance of brucite and related minerals for greenhouse gas removal. The reaction path involving carbonation of brucite ($Mg(OH)_2$) is particularly complex, as Mg has a strong tendency to form a series of metastable hydrous carbonates. These metastable hydrous carbonates include hydromagnesite ($Mg_5(CO_3)_4(OH)_2\cdot 4H_2O$, or $Mg_4(CO_3)_3(OH)_2\cdot 3H_2O$), artinite ($Mg_2CO_3(OH)_2\cdot 3H_2O$), nesquehonite ($Mg(OH)(HCO_3)\cdot 2H_2O$), and lansfordite ($MgCO_3\cdot 5H_2O$). The free energy of formation for these hydroxy and hydrous carbonates differ and their formation depends on the partial pressure of CO_2. The literature contains a number of methods for the synthesis of single phase nesquehonite and hydromagnesite. Various authors [11-15] have discussed the effects of temperature and partial pressure of carbon

dioxide p_{CO2} on the stability of the synthetic products. A thermal stability study conducted by Lanas *et al.* [16] discussed the inherent difficulty associated with studying the MgO-CaO-H$_2$O-CO$_2$ system as there are multiple complex minerals which can form during the dolomitization process.

Very few vibrational spectroscopic studies of the hydroxy carbonates have been forthcoming . Few Raman studies of any note are available [17, 18]. In this work the Raman spectra of a type hydromagnesite mineral is reported and related to the mineral structure and its formulation.

EXPERIMENTAL

Minerals

The mineral hydromagnesite (museum reference number M27404) was supplied by Museum Victoria and is a type mineral [19]. Where possible the phase purity of the minerals was checked by X-ray diffraction and the chemical composition by EDX measurements.

Raman microprobe spectroscopy

The crystals of hydromagnesite were placed and oriented on the stage of an Olympus BHSM microscope, equipped with 10x and 50x objectives and part of a Renishaw 1000 Raman microscope system, which also includes a monochromator, a filter system and a Charge Coupled Device (CCD). Raman spectra were excited by a HeNe laser (633 nm) at a nominal resolution of 2 cm^{-1} in the range between 100 and 4000 cm^{-1}. Details of the technique have been published by the authors.

Mid-IR spectroscopy

Infrared spectra were obtained using a Nicolet Nexus 870 FTIR spectrometer with a smart endurance single bounce diamond ATR cell. Spectra over the 4000–525 cm^{-1} range were obtained by the co-addition of 64 scans with a resolution of 4 cm^{-1} and a mirror velocity of 0.6329 cm/s. Spectra were co-added to improve the signal to noise ratio.

Spectral manipulation such as baseline adjustment, smoothing and normalisation were performed using the Spectracalc software package GRAMS (Galactic Industries Corporation,

NH, USA). Band component analysis was undertaken using the Jandel 'Peakfit' software package which enabled the type of fitting function to be selected and allows specific parameters to be fixed or varied accordingly. Band fitting was done using a Lorentz-Gauss cross-product function with the minimum number of component bands used for the fitting process. The Gauss-Lorentz ratio was maintained at values greater than 0.7 and fitting was undertaken until reproducible results were obtained with squared correlations of r^2 greater than 0.995.

RESULTS AND DISCUSSION

Spectroscopy of the carbonate anion

Nakamoto *et al.*. [20] first published and tabulated the selection rules for unidenate and bidentate anions including the carbonate anion. The free ion, CO_3^{2-} with D_{3h} symmetry exhibits four normal vibrational modes; a symmetric stretching vibration (v_1), an out-of-plane bend (v_2), a doubly degenerate asymmetric stretch (v_3) and another doubly degenerate bending mode (v_4). The symmetries of these modes are A_1' (R) + A_2'' (IR) + E´ (R, IR) + E´´ (R, IR) and occur at 1063, 879, 1415 and 680 cm^{-1} respectively. Generally, strong Raman modes appear around 1100 cm^{-1} due to the symmetric stretching vibration (v_1), of the carbonate groups, while intense IR and weak Raman peaks near 1400 cm^{-1} are due to the antisymmetric stretch (v_3). Infrared modes near 800 cm^{-1} are derived from the out-of-plane bend (v_2). Infrared and Raman modes around 700 cm^{-1} region are due to the in-plane bending mode (v_4). This mode is doubly degenerate for undistorted CO_3^{2-} groups. As the carbonate groups become distorted from regular planar symmetry, this mode splits into two components [37]. Infrared and Raman spectroscopy provide sensitive test for structural distortion of CO_3^{2-}.

Raman Spectroscopy

The Raman spectrum of hydromagnesite (reference sample M27404) in the 1050 to 1150 cm^{-1} spectral region is displayed in Fig. 1. A very intense band is found at 1121 cm^{-1} and is assigned to the v_1 CO_3^{2-} symmetric stretching mode. The band is slightly asymmetric on the lower wavenumber side and this band at 1102 cm^{-1} may be attributed to a hot band. Farmer [21] based upon the infrared spectra, reported two bands for the symmetric stretching mode at

1110 and 1120 cm^{-1}. In the infrared spectrum of hydromagnesite (Fig. 2), four bands may be resolved at 1387, 1413, 1474 and 1510 cm^{-1} attributed to the ν_3 CO$_3^{2-}$ antisymmetric stretching modes, with an additional band at 1654 cm^{-1} assigned to the water bending vibration of strongly hydrogen bonded water molecules. Farmer [21] reported three infrared bands at 1420, 1477 and 1515 cm^{-1}. The position of these later three bands agrees well with the infrared data reported here. The Raman spectrum of this spectral region (Fig. 3) is very noisy, nevertheless Raman bands are observed at 1451, 1490 and 1520 cm^{-1} which corresponds with the infrared bands above. In addition, Raman bands of low intensity are found at 1598, 1714 and 1768 cm^{-1}. These latter two bands may be due to the CO stretching vibration of HCO$_3^-$ units.   The band at 1598 cm^{-1} is assigned to a water bending mode.

The Raman spectrum of hydromagnesite in the 550 to 800 cm^{-1} region is shown in Fig. 4. The spectrum in this spectral region is complex with a series of overlapping bands. These are found at 708, 716, 728, 753 and 758 cm^{-1}. Farmer [21] reported infrared bands at 712, 730 and 743 cm^{-1}. The interpretation of these bands rests with a combination of HCO$_3^-$ and CO$_3^{2-}$ units. The Raman bands at 712, 728 and 743 cm^{-1} are assigned to the ν_4 CO$_3^{2-}$ bending modes. The series of bands at 644, 655, 673, 699 and 708 cm^{-1} are attributed to the ν_4 HCO$_3^-$ bending modes.

The Raman spectrum of hydromagnesite in the OH stretching region is reported in Fig. 5.   An intense Raman band is observed at 3516 cm^{-1} with a second band at 3447 cm^{-1}. These bands are assigned to the OH stretching vibration of the OH units in the hydromagnesite structure. The spectrum is strongly asymmetric on the low wavenumber side and an additional band at 3416 cm^{-1} may be resolved. In the infrared spectrum (Fig. 6), an intense band at 2940 cm^{-1} is attributed to water in the hydromagnesite structure. This band was not observed in the Raman spectrum. This is because water has a very low Raman scattering cross section. Intense infrared bands are observed at 3430, 3446, and 3511 cm^{-1}. These bands are assigned to the OH stretching vibrations of the OH units.

CONCLUSIONS

The concept of geosequestration involves the pumping of greenhouse gases to significant depths below the surface of the earth. The high partial pressure of CO$_2$ is

5

significant in that many different types of carbonates will be formed. Of significance are the magnesium carbonate minerals which will be formed by reaction of the liquefied CO_2 with magnesium minerals such as brucite and periclase. Among these minerals there is the possibility of the formation of hydromagnesite which are formed at reasonably low temperatures.

Raman spectroscopy has been used to characterise the mineral hydromagnesite and the bands related to the mineral structure. X-ray diffraction studies show the minerals can be disordered. This is reflected in the difficulty of obtaining spectra of reasonable quality and explains why the Raman spectra of these minerals have not been previously or sufficiently described. The minerals are characterised by CO_3^{2-} v_1 symmetric stretching modes but very weak antisymmetric stretching and bending modes.

Acknowledgments

REFERENCES

[1]   O. S. Pokrovskii, *Litologiya i Poleznye Iskopaemye* **1996,** 531-540.

[2]   F. L. Sayles, W. S. Fyfe, *Geochim. Cosmochim. Act.* **1973,** *37,* 87-99.

[3]   S. Iro, J. Sevc, *Acta Geol.Univ. Comenianae* **2000,** *55,* 73-80.

[4]   G. Baron, S. Caillere, R. Lagrange, T. Pobeguin, *Bull. Soc. Franc.* **1959,** *82,* 150-158.

[5]   A. R. Alderman, *Geochim. Cosmochim. Act.* **1965,** *29,* 1355-1366.

[6]   E. C. Kirchner, P. Simonsberger, *Karinthin* **1982,** *87,* 395-400.

[7]   R. Brousse, A. Lambert, F. Chantret, *Comptes Rendus* **1975,** *95,* 207-214.

[8]   R. Fischbeck, G. Mueller, *Contrib. Miner. Petr.* **1971,** *33,* 87-92.

[9]   V. C. Whitehead, T. C. Keener, S.-J. Khang, *Proceedings of the Air & Waste Management Association's Annual Conference & Exhibition, 93rd, Salt Lake City, UT, United States, June 18-22, 2000* **2000,** 5437-5446.

[10]   S. W. M. Blake, C. Cuff, Preparation and use of cationic halides, sequestration of carbon dioxide. (Perma-Carb Pty Ltd, Australia). Application: WO 2007, p. 66pp.

[11]   Magnesium carbonate in the form of nesquehonite or lansfordite. (Basic Refractories Inc.). G, 1946.

[12]   G. Cesaro, *Bull. Acad. Roy. Belg.* **1910,** 844-845.

[13]   G. Cesaro, *Bull. Acad. Roy. Belg.* **1910,** 749-768.

[14]   E. D. Glover, R. F. Sippel, *Geochim. Cosmochim. Act.* **1967,** *31,* 603-613.

[15]   B. Valuziene, A. Kaminskas, K. Gasiunas, *Sb. Tr. VNII Teploizolyats. i Akust. Stroit. Materialov i Izdelii* **1976,** 183-188.

[16]   J. Lanas, J. I. Alvarez, *Thermochim. Act.* **2004,** *421,* 123-132.

[17]   H. Fan, K. Tao, Y. Xie, K. Wang, *Yanshi Xuebao* **2003,** *19,* 169-172.

[18]   W. Hong, S. He, S. Huang, Y. Wang, H. Hou, X. Zhu, *Guangpuxue Yu Guangpu Fenxi* **1999,** *19,* 546-549.

[19]   J. W. Anthony, R. A. Bideaux, K. W. Bladh, M. C. Nichols, Handbook of Mineralogy, Mineral Data Publishing, Tuscon, Arizona, USA, 2003.

[20]   K. Nakamoto, Infrared Spectra of Inorganic and Coordination Compounds, Wiley, London1963.

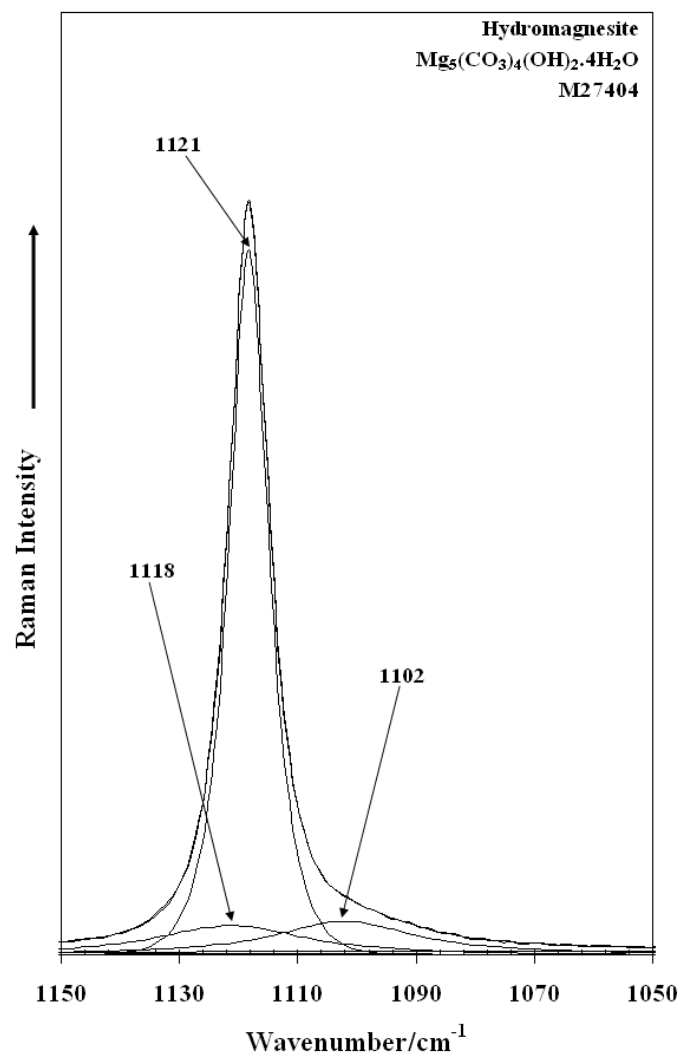[21]   V. C. Farmer, Mineralogical Society Monograph 4: The Infrared Spectra of Minerals, Published by The Mineralogical Society, London, 1974.

List of Figures

Fig. 1

Fig. 2

Fig. 3

Hydromagnesite
$Mg_5(CO_3)_4(OH)_2 \cdot 4H_2O$
M27404

Fig. 4

Fig. 5

Hydromagnesite
Mg$_5$(CO$_3$)$_4$(OH)$_2$·4H$_2$O
M27404

Fig. 6 INFRARED